Available online at www.sciencedirect.com

ScienceDirect

journal homepage: www.elsevier.com/locate/issn/15375110

Research Paper

A mechanistic thermal balance model of dairy cattle

Jinghui Li [a], *Vinod Narayanan* [b], *Ermias Kebreab* [a], *Serdal Dikmen* [c], *James G. Fadel* [a,*]

[a] Department of Animal Science, University of California, Davis, CA 95616, USA
[b] Department of Mechanical and Aerospace Engineering, University of California, Davis, CA 95616, USA
[c] Faculty of Veterinary Medicine, Department of Animal Science, Bursa Uludag University, Bursa, 16059, Turkey

ARTICLE INFO

Article history:
Received 10 December 2020
Received in revised form
10 June 2021
Accepted 11 June 2021

Keywords:
Dairy cow
Thermal balance model
Heat stress

A dynamic model describing the thermal balance of Holstein dairy cattle was developed. The model quantified the heat flow of five main nodes at the body core, top and bottom skin, and top and bottom coat of a dairy cow. Heat production by the animal and heat flows between the animal and the environment, including conduction, convection, evaporation and radiation, were calculated based on existing models and physical principles. The model requires information of climate, animal characteristics and location as inputs, and returns body core, skin and coat temperatures as outputs. The thermal balance model was evaluated through two datasets. The root mean squared error of prediction for body temperature was 1.16 °C and 0.40 °C for the two datasets, respectively. A simulation study was conducted based on a Holstein dairy cow with 600 kg of body weight and 25 kg of daily milk yield under a typical summer environment in California, USA for three days. The average simulated temperatures of body, top and bottom skin, and top and bottom coat were 40.9, 35.6, 35.9, 34.1 and 33.7 °C, respectively. A local and a global sensitivity analyses showed that heat production, surface area and the parameters relative to respiration and sweating were the most sensitive. The model is able to predict the dynamic change of body temperature under hot weather, and to guide the use of physical cooling strategies, such as shade, fans, sprinklers and cooling mats in dairy facilities.

© 2021 The Authors. Published by Elsevier Ltd on behalf of IAgrE. This is an open access article under the CC BY-NC-ND license (http://creativecommons.org/licenses/by-nc-nd/4.0/).

1. Introduction

Thermal stress is a major factor that can cause losses in production of dairy cows, who prefer an ambient temperature between 5 and 25 °C (Roenfeldt, 1998). Heat stress can be defined as the sum of external forces (dry bulb temperature, humidity, wind speed and radiation) that act to displace the body temperature on animals from ground state (Hansen et al., 2020). Heat stress negatively affects the health of animals through their physiology (Lacetera et al., 1996), metabolism (Nardone et al., 2010) and immune system (Das et al., 2016), resulting in decreased production. Temperature humidity index (THI), calculated using air temperature and relative humidity, has been used as a way to

* *Corresponding author*. Department of Animal Science, University of California, 2115 Meyer Hall, Davis, CA 95616, USA.
E-mail addresses: lgreyhui@hotmail.com (J. Li), vnarayanan@ucdavis.edu (V. Narayanan), ekebreab@ucdavis.edu (E. Kebreab), serdal@uludag.edu.tr (S. Dikmen), jgfadel@ucdavis.edu (J.G. Fadel).
https://doi.org/10.1016/j.biosystemseng.2021.06.009
1537-5110/© 2021 The Authors. Published by Elsevier Ltd on behalf of IAgrE. This is an open access article under the CC BY-NC-ND license (http://creativecommons.org/licenses/by-nc-nd/4.0/).

Nomenclature

Symbol	Description
A	Animal surface area, m^2
Ah/A	The ratio of shadow area to body area
BW	Animal body weight, kg
c_h	Heat production coefficient, 44.1 for high production cows (milk yield $\geq$ 30 kg/d), 38.7 for intermediate production cows (milk yield < 30 kg d^{-1}) and 29.7 for dry cows
c_{pb}	Specific heat capacity of body core, 3472, J kg^{-1} K^{-1}
c_{pc}	Specific heat capacity of coat, 1006.43, J kg^{-1} K^{-1}
c_{ps}	Specific heat capacity of skin, 3472, J kg^{-1} K^{-1}
c_{psoil}	Specific heat of soil, 1784, J kg^{-1} K^{-1}
D	Diffusion coefficient of water vapor in air, m^2 s^{-1}
d_a	Laminar thickness, m
d_c	Coat thickness, 0.0025, m
d_h	Hair diameter, 0.0625, mm
d_i	Distance between two nodes underground, 0.01, m
HE	Heat production rate, W
h_c	Convection coefficient, W m^{-2} K^{-1}
h_m	Mass transfer coefficient, m s^{-1}
k_a	Air conductivity, 0.024, W m^{-1} k^{-1}
k_{eff}	Effective thermal conductivity, W m^{-1} K^{-1}
k_f	Fur conductivity, 0.26, W m^{-1} k^{-1}
k_{soil}	Soil conductivity, 1,64, W m^{-1} k^{-1}
k_x	Horizontal thermal conductivity, W m^{-1} K^{-1}
k_y	Vertical thermal conductivity, W m^{-1} K^{-1}
M_b	Body core mass, kg
M_c	Coat mass, kg
ME	Metabolizable energy intake, J
M_s	Skin mass, kg
p_c	Proportion of contact surface to the whole animal surface area, 0.2
$q''_{cond,\ b\text{-}s1}$	Heat conduction between body core and top skin, W m^{-2}
$q''_{cond,\ b\text{-}s2}$	Heat conduction between body core and bottom skin, W m^{-2}
$q''_{cond,\ i}$	Heat conduction flux at node i underground, W m^{-2}
$q''_{cond,\ s1\text{-}c1}$	Heat conduction between top skin and top coat, W m^{-2}
$q''_{cond,\ s2\text{-}c2}$	Heat conduction between bottom skin and bottom coat, W m^{-2}
$q''_{cond,\ s2\text{-}g}$	Heat conduction between bottom skin and ground, W m^{-2}
q''_{conv1}	Heat convection at top coat surface, W m^{-2}
q''_{conv2}	Heat convection at bottom coat surface, W m^{-2}
q''_{evap1}	Heat evaporation through sweating at top skin, W m^{-2}
q''_{evap2}	Heat evaporation through sweating at bottom skin, W m^{-2}
q''_{lat}	Latent heat transfer, W m^{-2}
q''_{lw1}	Long wave radiation at top coat, W m^{-2}
q''_{lw2}	Long wave radiation at bottom coat, W m^{-2}
q''_{resp}	Heat loss through respiration, W m^{-2}
q''_{sen}	Sensible heat transfer, W m^{-2}
q''_{sol1}	Solar radiation at top coat, W m^{-2}
q''_{sol2}	Solar radiation at bottom coat, W m^{-2}
RE	Retained energy, J
RR	Respiration rate, breath s^{-1}
r_{sg}	Heat conduction resistance between the skin and the ground surface, 0.1, m^2 K W^{-1}
r_{s1}	Skin resistance, m^2 K W^{-1}
S_b	Direct radiation, W m^{-2}
S_d	Diffuse radiation, W m^{-2}
T_a	Air temperature, K
T_{adl}	Temperature at the adiabatic layer, K
T_b	Body temperature, K
T_{black}	Black globe temperature, K
T_{c1}	Top coat temperature, K
T_{c2}	Bottom coat temperature, K
T_g	Ground surface temperature, K
$T_{g,\ i}$	Ground temperature at node i, for i = 1, …, 50, K
T_r	Radiant temperature of environment, K
T_{s1}	Top skin temperature, K
T_{s2}	Bottom skin temperature, K
T_{sky}	Sky temperature, K
Tv_a	Virtual temperature of inhaled air, K
Tv_e	Virtual temperature of exhaled air, K
u	Wind speed, m s^{-1}
V_t	Tidal volume, m^3 $breath^{-1}$
ε_c	Emissivity of coat, 0.98
λ	Latent heat of vaporisation of water, 2430, J g^{-1}
ρ_c	Reflection coefficient of coat, 0.3
ρc_p	Volumetric heat capacity of air, J m^{-3} K^{-1}
ρ_g	Reflection coefficient of ground, 0.25 for grass, 0.08 for wet dark soil, 0.13 for dry dark soil, 0.10 for wet light soil and 0.18 for dry light soil
ρ_h	Fur density, 9.87, hairs mm^{-2}
ρ_{soil}	Soil density, 1559, kg m^{-3}
σ	Stefan–Boltzmann constant, 5.67 × 10^{-8}, W m^{-2} K^{-4}
χ_a	Absolute humidity of inhaled air, g m^{-3}
χ_e	Absolute humidity of exhaled air, g m^{-3}
χ_{s1}	Absolute humidity of top skin surface, g m^{-3}

express heat stress experienced by animals (Mader et al., 2006). However, THI evaluates the thermal environment instead of the thermal condition of the animal, therefore it is not accurate enough to evaluate thermal stress. Body temperature of dairy cattle shows great susceptibility to hot weather (Araki et al., 1984), which makes it a more sensitive indicator of thermal stress. When the body temperature is over 39 °C under hot weather conditions, cows are likely to be in heat stress (Zimbelman et al., 2009). It has been suggested that milk production significantly decreases when rectal temperature is over 39 °C for more than 16 h (Igono et al., 1992), with 1.8 kg of production decline for every 0.55 °C increase in rectal temperature (West, 2003). Increase of body temperature also depresses the conception rate (Nabenishi et al., 2011) and cause severe damage on follicles when body temperature is over 40 °C (Roth et al., 2000).

Many attempts have been made to investigate the heat flow and temperature change of dairy cows under different climate

conditions. Some studies have focused on certain types of heat transfer mechanisms, including evaporative cooling (Berman, 2006; Gebremedhin et al., 2001; Maia et al., 2005), respiratory heat loss (da Silva et al., 2002; Maia & Loureiro, 2005) and solar radiation (Yamamoto et al., 1994). However, this approach does not connect heat transfer with body temperature. McArthur (1987) developed a comprehensive model describing the thermal interaction between animal and microclimate, which was modified by Turnpenny et al. (2000a), but their model was not evaluated thoroughly and can only predict body temperature under a static environment (i.e., where environmental conditions do not change). Thompson et al. (2014a) developed a thermal balance model for beef cattle by connecting the heat flows with body temperature. Their model structure allows for the prediction of dynamic body temperature under a constantly changing environment, thus was used in this study. Here we aim to develop a thermal balance model for dairy cows in order to understand the thermal conditions of the animal and to improve the heat mitigation strategies under hot climate.

2. Model description

The most important difference between our model and previous ones (McGovern & Bruce, 2000; Thompson, Barioni, Rumsey, Fadel, & Sainz, 2014a; Turnpenny et al., 2000a) is that our model includes heat conduction between the animal and the ground surface when the animal lies down, whilst previous models do not. Although cows in heat stress tend to stand rather than lie down (Chen et al., 2016; Shultz, 1984), lying down still accounts for about one third of the total time budget for dairy cows in summer (Cook et al., 2007), therefore it is necessary to consider it.

The heat balance model developed in this study requires climate information (Julian day number, air temperature, relative humidity, wind speed and annual average air temperature), animal information (body weight, milk production, feed intake and feed ingredients), location (latitude and altitude) and timing of behaviours (lying down and standing up) as inputs for animals outdoor, and returns body core, skin and coat temperatures as outputs. Black globe temperature is required as an additional input for animals located indoor. The temperatures of body core, skin and coat were calculated in absolute units (Kelvin) in the model but converted to Celsius degree in the simulation result for ease of understanding. The model and all the analyses were coded in R statistical software (Version 3.5.3, R Core Team, 2019). The FME package (Soetaert & Petzoldt, 2010) was used to solve the differential equations.

2.1. *Differential equations*

A heat balance model with five main nodes (the surface layer of body core, top and bottom skin and, top and bottom coat) was developed. A similar model structure was adopted in previous studies (McGovern & Bruce, 2000; Thompson et al., 2014a) to represent different temperatures and thermal properties (conductivity, specific heat, etc.) of each node. The skin and coat were divided into top and bottom parts to account for different heat transfer mechanisms occurring in these regions when the animal lies down, with the bottom skin and coat representing the part in contact with the ground surface and the top part representing the rest. The geometry of the nodes is represented by three concentric cylinders (top and bottom skin and coat consist of two cylinders), and the control volume surrounding each node has uniform internal temperature and thermal properties. The temperature of each node is regulated by different heat flows as shown in Fig. 1. The dynamic change of heat at each node results in temperature changes. For the body core node, the heat flows include heat production by the animal, heat dissipation through respiration, and heat conduction between body core and skin. For the top skin node, the heat flows include heat conduction between body core and skin, heat conduction between skin and coat, and heat dissipation through evaporation. The bottom skin node shares the same heat flows as the top one when the animal stands up. When the animal lies down, we assumed that evaporation does not happen at the bottom skin, therefore the heat flows include the conduction between body core and skin and the conduction between skin and ground surface. For the top coat node, the heat flows include solar radiation, heat conduction between skin and coat, heat convection at the coat surface, and long wave radiation between the coat and the surrounding. The bottom coat node has the same heat flows as the top coat when the animal stands up. When the animal lies down, no heat transfer was considered for the bottom coat, and we assumed that it has the same temperature as bottom skin. Besides, we also assumed that no heat transfer occurs between top and bottom skin, or between top and bottom coat. Heat flows are in the unit of W to represent heat transfer rate in Fig. 1 and can be converted to heat flux (Wm^{-2}) by dividing by the surface area to represent the heat transfer rate per unit of area. Five differential equations representing the dynamic heat and temperature change of body core, top and bottom skin, and top and bottom coat can be developed based on the nodal energy balances as follows:

Body core node:

$$d\left(M_b c_{pb} T_b\right) / dt = HE - A\left[p_c q''_{cond,\ b-s1} + \left(1-p_c\right) q''_{cond,\ b-s2} + q''_{resp}\right] \tag{1}$$

Top skin node:

$$d\left[\left(1-p_c\right) M_s c_{ps} T_{s1}\right] \Big/ dt = \left(1-p_c\right) A\left(q''_{cond,b-s1} - q''_{cond,s1-c1} - q''_{evap1}\right) \tag{2}$$

Bottom skin node:

$$d\left(p_c\ M_s\ c_{ps}\ T_{s2}\right)/dt\ = \begin{cases} p_c\ A\left(q''_{cond,\ b-s2} - q''_{cond,\ s2-c2} - q''_{evap2}\right) \text{ standing up} \\ p_c\ A\left(q''_{cond,\ b-s2} - q''_{cond,\ s2-g}\right) \text{ lying down} \end{cases} \tag{3}$$

Top coat node:

$$d\left[\left(1-p_c\right) M_c c_{pc} T_{c1}\right] / dt = \left(1-p_c\right) A\left(q''_{cond,s1-c1} + q''_{sol1} - q''_{conv1} - q''_{lw1}\right) \tag{4}$$

Bottom coat node:

$$d\left(p_c\ M_c\ c_{pc}\ T_{c2}\right)/dt\ = \begin{cases} p_c\ A\left(q''_{cond,\ s2-c2} + q''_{sol2} - q''_{conv2} - q''_{lw2}\right) \text{ standing up} \\ 0, \text{ lying down} \end{cases} \tag{5}$$

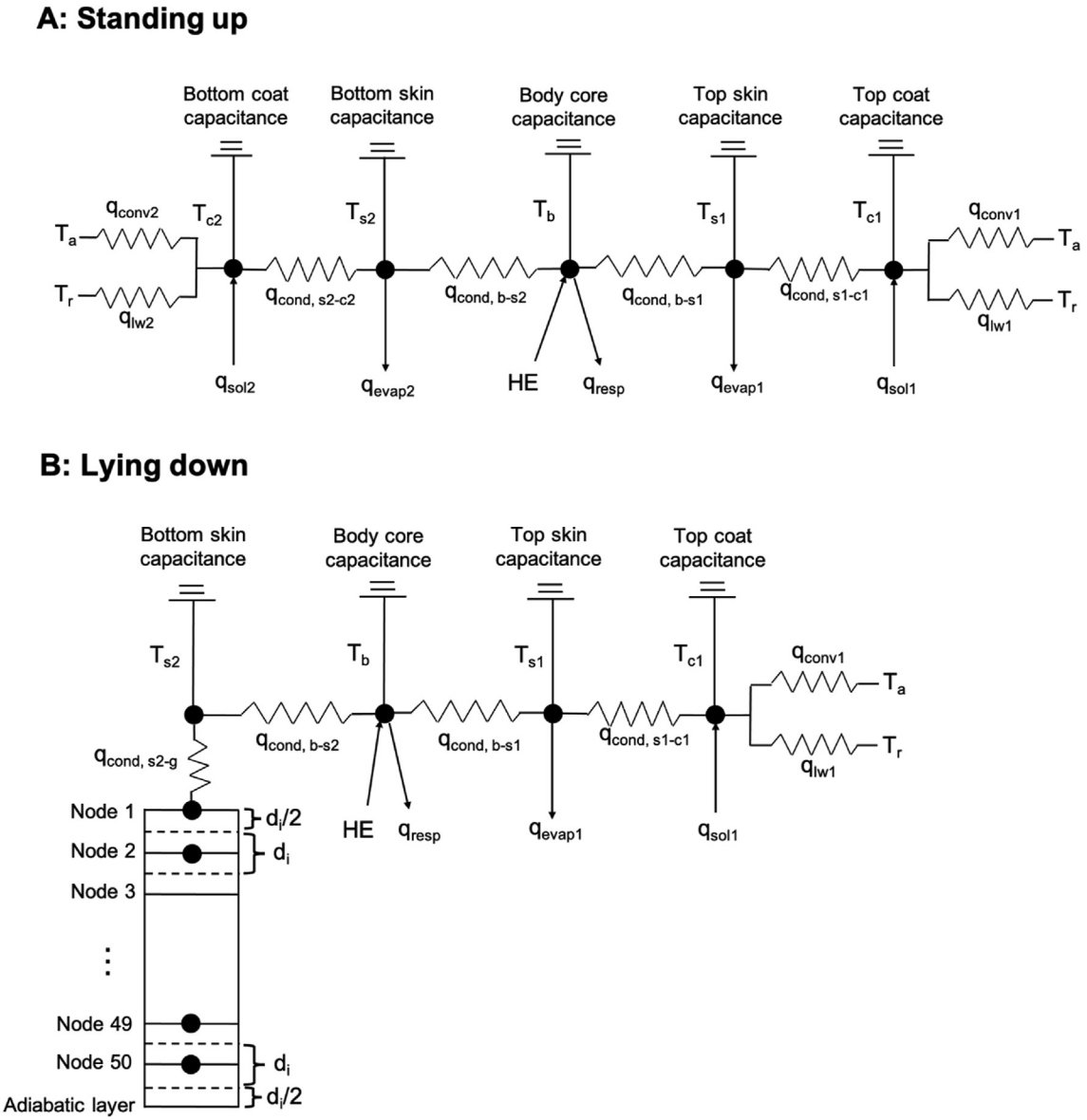

Fig. 1 – The thermal network diagram of the heat balance model for a dairy cow standing (A) up and lying down (B). T_b = Body temperature, T_{s1} = Top skin temperature (K), T_{s2} = Bottom skin temperature (K), T_{c1} = Top coat temperature (K), T_{c2} = Bottom coat temperature (K), T_a = Air temperature (K), T_r = Surrounding radiant temperature (K), HE = Heat production (W), q_{resp} = Heat dissipation through respiration (W), $q_{cond,\ b\text{-}s1}$ = Heat conduction between body core and top skin (W), $q_{cond,\ b\text{-}s2}$ = Heat conduction between body core and bottom skin (W), q_{evap1} = Heat dissipation through evaporation through sweating at the top skin (W), q_{evap2} = Heat dissipation through evaporation through sweating at the bottom skin (W), $q_{cond,\ s1\text{-}c1}$ = Heat conduction between top skin and top coat (W), $q_{cond,\ s2\text{-}c2}$ = Heat conduction between bottom skin and top coat (W), q_{sol1} = Solar radiation at the top coat (W), q_{sol2} = Solar radiation at the bottom coat (W), q_{conv1} = Heat convection at the top coat surface (W), q_{conv2} = Heat convection at the bottom coat surface (W), q_{lw1} = Long wave radiation between the top coat and surrounding (W), q_{lw2} = Long wave radiation between the bottom coat and surrounding (W), $q_{cond,\ s2\text{-}g}$ = Heat conduction between bottom skin and ground surface (W). For each node, the capacitance is able to store and dissipate heat with time, which brings about transient temperature changes. The arrow indicates the one-way direction of heat flows (HE, q_{resp}, q_{evap1}, q_{evap2}, q_{sol1} and q_{sol2}), while the other heat flows can happen in either direction to or from the node. When the animal lies down (B), the vertical distance from the bottom skin to adiabatic layer is divided into 50 nodes, with the distance between each of two nodes d_i equal to 0.01 m, and the dashed lines represent the centre of each control volume. The bottom coat capacitance was not accounted and T_{s2} is the same as T_{c2} when the animal lies down.

where A (m^2) is animal surface area; M_b, M_s and M_c (kg) are the mass of body core, skin and coat, respectively; c_{pb}, c_{ps} and c_{pc} (J kg^{-1} K^{-1}) are the specific heat capacity of body core, skin and coat, respectively; T_b, T_{s1}, T_{s2}, T_{c1} and T_{c2} (K) are the temperature of body core, top skin, bottom skin, top coat and bottom coat, respectively; p_c (–) is the proportion of contacting surface to the animal surface area when the animal lies down, taken equal to 0.2 (Ortiz et al., 2015); *HE* (W) is the heat production by animal; $q''_{cond,\ b\text{-}s1}$ and $q''_{cond,\ b\text{-}s2}$ (W m^{-2}) are heat conduction between body core and top and bottom skin, respectively; q''_{resp} (W m^{-2}) is heat loss through respiration; $q''_{cond,\ s1\text{-}c1}$ and $q''_{cond,\ s2\text{-}c2}$ (W m^{-2}) are heat conduction between top skin and coat and between bottom skin and coat, respectively; q''_{evap1} and q''_{evap2} (W m^{-2}) are heat evaporation through sweating at top and bottom skin, respectively; $q''_{cond,\ s2\text{-}g}$ (W m^{-2}) are heat conduction between bottom skin and ground surface; q''_{sol1} and q''_{sol2} (W m^{-2}) is solar radiation at top and bottom coat, respectively; q''_{conv1} and q''_{conv2} (W m^{-2}) are heat convection at top and bottom coat, respectively; q''_{lw1} and q''_{lw2} (W m^{-2}) are the net heat flux from the animal to the environment through long wave radiation at top and bottom coat, respectively. One should note that all the heat transfer routes could occur in both directions depending on the temperature difference between two surfaces, except for evaporation and solar radiation. For example, $q''_{cond,\ b\text{-}s1}$ is subtracted in Eq. (1) to indicate a heat outflow from the body core, which is true when the body temperature is higher than the top skin temperature, but when the top skin temperature is higher, $q''_{cond,\ b\text{-}s1}$ is negative and becomes a heat inflow from top skin to body core.

The condensed model equations are shown below, and detailed description of the model equations is presented in Supplementary file 1. The differential equations allow for solving the five unknowns, T_b, T_{s1}, T_{s2}, T_{c1} and T_{c2} after quantifying all the other variables.

2.2. Heat production by the animal

The average daily heat production (HE, W) can be calculated as:

$$HE = (ME - RE)/86,400 \tag{6}$$

where *ME* is daily metabolisable energy intake (J); *RE* is daily retained energy (J); 86,400 is the amount of time (s) per day. Given the feed ingredients of a diet, feed intake, milk production and body weight change, *ME* and *RE* can be estimated based on NRC (2001). Heat production can also be roughly estimated through an empirical equation (Purwanto et al., 1990) when detailed dietary information is not available:

$$HE = c_h\, BW^{0.75}/3.6 \tag{7}$$

where c_h (–) is the heat production coefficient equal to 44.1 for high production cows (daily milk yield ≥ 30 kg), 37.8 for intermediate production cows (daily milk yield < 30 kg) and 29.7 for dry cows. Some researchers have claimed that drinking cold water helps with heat mitigation in summer (Bewley et al., 2008) whilst others only found transient effect of cold water (Baker et al., 1988). The heat mitigation through drinking water was approximated by assuming a cow drinking 100 l of 25 °C water per day and heating all of it up to the body temperature (38.5 °C). All water consumed would be lost through manure, milk or sweat. Thus, the amount of heat absorbed by the consumed water (~5.6×10^6 J) is less than 1% of the total heat production by the animal based on our calculation, therefore the cooling effect of drinking water was not considered in the model.

2.3. Heat conduction between body core and skin

Heat conduction between body core and top skin surface ($q''_{cond,\ b\text{-}s1}$, W m^{-2}) can be calculated based on McArthur (1987):

$$q''_{cond,\ b-s1} = \rho c_p (T_b - T_{s1}) / r_{s1} \tag{8}$$

where ρc_p (J m^{-3} K^{-1}) is volumetric heat capacity of air and r_{s1} (s m^{-1}) is skin resistance. Skin resistance is a function of T_{s1}, reflecting the change of skin conductivity in response to heat stress (McArthur, 1987):

$$r_{s1} = max(-5.44(T_{s1} - 273.15) + 225,\ 29) \tag{9}$$

where 29 s m^{-1} is the minimum of skin resistance. The conduction between body core and bottom skin surface can be calculated by replacing T_{s1} with T_{s2} in Eqs. (8) and (9)

2.4. Heat loss through respiration

Heat loss through respiration (q''_{resp}, W m^{-2}) consists of sensible heat transfer (q''_{sen}, W m^{-2}) and latent heat transfer (q''_{lat}, W m^{-2}):

$$q''_{resp} = q''_{sen} + q''_{lat} \tag{10}$$

Sensible heat transfer occurs between inhaled air and exhaled air due to temperature difference, whilst latent heat transfer occurs due to the transformation of water from liquid to vapour in the lung without temperature change. The equations are described as follows (McGovern, 2000; Monteith & Unsworth, 2013):

$$q''_{sen} = V_t RR \rho c_p (Tv_e - Tv_a) / A \tag{11}$$

$$q''_{lat} = \lambda V_t RR (\chi_e - \chi_a) / A \tag{12}$$

where V_t (m^3 $breath^{-1}$) is tidal volume; *RR* (breath s^{-1}) is respiration rate; Tv_e (K) and Tv_a (K) are virtual temperatures of exhaled air and inhaled air, respectively; λ (2430 J g^{-1}) is the latent heat of vaporisation of water (Monteith & Unsworth, 2013); A (m^2) is area of animal body surface; χ_e (g m^{-3}) and χ_a (g m^{-3}) are absolute humidity of exhaled air and inhaled air, respectively.

2.5. Heat conduction between skin and coat

Heat conduction between top skin and top coat ($q''_{cond,\ s1\text{-}c1}$, W m^{-2}) is calculated as:

$$q''_{cond,\ s1-c1} = k_{eff} (T_{s1} - T_{c1}) / d_c \tag{13}$$

where k_{eff} (W m^{-1} K^{-1}) is the effective thermal conductivity of coat, and d_c (0.0025 m) is the coat thickness (Bertipaglia et al., 2005). Coat layer is a mixture of fur and air, the thermal conductivity for which is derived by Gebremedhin et al. (2001) as:

$$k_{eff} = 0.5(k_x + k_y) \tag{14}$$

$$k_x = \left(\rho_h \pi {d_h}^2 / 4\right) k_f + \left(1 - \rho_h \pi {d_h}^2 / 4\right) k_a \tag{15}$$

$$k_y = k_a \left(1 / {\rho_h}^{0.5} - d_h\right) {\rho_h}^{0.5} + d_h k_a k_f / \left(d_h k_a + \left(1 / {\rho_h}^{0.5} - d_h\right) k_f\right) \tag{16}$$

where k_x (W m^{-1} K^{-1}) is horizontal thermal conductivity; k_y (W m^{-1} K^{-1}) is vertical thermal conductivity; ρ_h (9.87 hairs mm^{-2}) is fur density (Bertipaglia et al., 2005); d_h (0.0625 mm) is hair diameter (Bertipaglia et al., 2005); k_f (0.26 W m^{-1} K^{-1}) is fur conductivity (Gebremedhin et al., 2016); k_a (0.024 W m^{-1} K^{-1}) is air conductivity. Based on the above parameter values, k_{eff} = 0.028 W m^{-1} K^{-1}. The conduction between bottom skin and bottom coat can be calculated by replacing T_{s1} and T_{c1} with T_{s2} and T_{c2} in Eq (13).

2.6. Heat evaporation through sweating

Heat loss through sweating is limited by either sweating rate or potential evaporation rate, which is dependent on the environmental conditions (Thompson et al., 2014a). Therefore, the minimum value of two functions (Gebremedhin & Wu, 2001; Silva & Maia, 2011) based on sweating rate and potential evaporation rate is used to represent the heat evaporation at the top skin (q''_{evap1}, W m^{-2}):

$$q''_{evap1} = min(31.5 + 3.67exp [(T_{s1} - 301.05) / 2.19],\ \lambda(\chi_{s1} - \chi_a) / [1 / h_m + (d_c + d_a) / D]) \tag{17}$$

where χ_{s1} (g m^{-3}) is absolute humidity at the top skin; χ_a (g m^{-3}) is absolute humidity of air, which is the same as the absolute humidity of inhaled air in equation 4.3; h_m (m s^{-1}) is mass transfer coefficient; d_a (m) is laminar thickness; D (m^2 s^{-1}) is diffusion coefficient of water vapour in air. The first part is an empirical equation representing q''_{evap1} through sweating rate based on T_{s1}, whilst the second part describes the potential evaporation rate based on the environmental air conditions. Heat evaporation at the bottom skin can be calculated by replacing T_{s1} with T_{s2} in Eq. (17).

2.7. Heat convection at coat surface

Conduction occurs between two still surface whilst convection occurs between a still surface and a fluid in motion, therefore the heat transfer between coat surface and air is considered as convection. Heat convection at the top coat surface (q''_{conv1}, W m^{-2}) can be expressed using Newton's law of cooling as:

$$q''_{conv1} = h_c(T_{c1} - T_a) \tag{18}$$

where h_c (W m^{-2} K^{-1}) is the convection heat transfer coefficient, which is a function of Nusselt number and surface properties (Monteith & Unsworth, 2013). The calculation of Nusselt number is based on Reynolds number, which is dependent on the nature of the fluid motion, surface geometry and the various fluid thermodynamic properties (Gebremedhin & Wu, 2001). The convection at the bottom coat can be calculated by replacing T_{c1} with T_{c2} in Eq. (18).

2.8. Heat flux through long wave radiation

Thermal radiation is the energy emitted by matter that is at a nonzero absolute temperature. The radiation between the top coat surface and surroundings (q''_{lw1}, W m^{-2}) has longer wavelength than solar radiation, and can be prescribed by the Stefan–Boltzmann law:

$$q''_{lw1} = \sigma\varepsilon_c({T_{c1}}^4 - {T_r}^4) \tag{19}$$

where σ (5.67 × 10^{-8} W m^{-2} K^{-4}) is Stefan–Boltzmann constant; ε_c (0.98, –) is the emissivity of coat (Maia & Loureiro, 2005); T_r (K) is the average radiant temperature of the surrounding. When the animal is outdoor, T_r is calculated as the average of sky temperature (T_{sky}, K) and ground temperature (T_g, K):

$$T_r = (T_{sky} + T_g) / 2 \tag{20}$$

Similarly, when the animal is indoor, T_r can be calculated as the average of roof temperature and floor temperature. However, estimating roof temperature is difficult, therefore indoor T_r is estimated through black globe temperature (Kuehn et al., 1970; Thorsson et al., 2007):

$$T_r = \left({T_{black}}^4 + 1.1 \times 10^{-8} u^{0.6}(T_{black} - T_a)/2.029\right)^{0.25} \tag{21}$$

where T_{black} (K) is black globe temperature and u (m s^{-1}) is wind speed. The long radiation between the bottom coat and surroundings can be calculated by replacing T_{c1} with T_{c2} in Eq. (19).

2.9. Heat flux through solar radiation

Solar radiation is an important heat input to animals when exposed to the sun. Turnpenny et al. (2000a) divided heat flux through solar radiation (q''_{sol}, W m^{-2}) into three parts, including direct and diffusive radiation from the sun, and the radiation reflected by the ground:

$$q''_{sol} = (1 - \rho_c)\left[(A_h / A)S_b + 0.5S_d + 0.5\rho_g(S_b + S_d)\right] \tag{22}$$

where ρ_c (0.3, -) is the reflection coefficient of coat (Turnpenny et al., 2000b); A_h/A (–) is the proportion of body surface the receives the direct solar radiation, taking the orientation of the animal and the solar altitude angle into account; S_b (W m^{-2}) is the direct radiation from the sun; S_d (W m^{-2}) is the diffusive radiation from the sun; ρ_g (–) is the reflection coefficient of ground. The coefficient 0.5 represents the assumption that half of the body surface faces towards the sky and receives diffusive solar radiation, while the other half faces towards the ground and receives the reflected radiation from the ground. Then the heat flow through solar radiation (q_{sol}, W) received by the animal is:

$$q_{sol} = A q''_{sol} \tag{23}$$

Since the coat was divided into top and bottom parts in this study, the equation was modified to quantify the solar radiation at the top (q_{sol1}, W) and bottom coat (q_{sol2}, W) separately:

$$q_{sol1} = A(1-\rho_c)(A_h/A)S_b + 0.5S_d + (0.5-p_c)A\rho_g(S_b+S_d) \quad (24)$$

$$q_{sol2} = p_c A\rho_g(S_b+S_d) \quad (25)$$

It was assumed that the direct radiation and diffusive radiation are received by the top coat, and that the bottom coat only receives the reflected radiation from the ground. Since the proportion of bottom coat to the total coat ($p_c = 0.2$) is < 0.5, the rest of the reflected radiation from the ground is received by the top coat. Thus, the heat flux of solar radiation in Eqs. (4) and (5) can be calculated by dividing the heat flow by the area:

$$q''_{sol1} = q_{sol1} / [(1-p_c)A] \quad (26)$$

$$q''_{sol2} = q_{sol2}/p_c A \quad (27)$$

Solar radiation is affected by cloud (Hottel, 1976), which was not considered in this study. Cloudiness is difficult to quantify and is highly variable. It was considered better to obtain solar radiation through direct measurement instead of estimation on cloudy days.

2.10. *Heat conduction between animal and ground when lying down*

A finite difference method (Bastian et al., 2003) was used to quantify the heat conduction between the animal and the ground through dividing the vertical distance between contacting surface and an adiabatic layer underground into many small nodes. The adiabatic layer was estimated using thermal penetration depth 2.3 $(\alpha_{soil}\, t)^{0.5}$ (Bergman et al., 2011), where α_{soil} ($m^2\ s^{-1}$) is the thermal diffusivity and t (s) is the time after lying down. In this study, a soil type of heavy clay with thermal diffusivity equal to 5.9×10^{-7} $m^2\ s^{-1}$ (Najib et al., 2020) was assumed. To estimate the thermal penetration conservatively, the undisturbed depth was set to be 0.5 m when the animal lies down for the whole day (t = 86,400 s). The vertical distance from the contact surface to the adiabatic layer was divided into 50 nodes, with the distance of d_i equal to 0.01 m between each of two nodes (Fig. 1). The heat conduction ($q''_{cond,\ 1}$, $W\ m^{-2}$) into the first node, i.e., the conduction between the animal and the ground surface ($q''_{cond,\ s2\text{-}g}$), was calculated by (Radoń et al., 2014):

$$q''_{cond,\ s2-g} = (T_{s2} - T_{g,\ 1}) \Big/ r_{sg} \quad (28)$$

where $T_{g,\ 1}$ (K) is the ground temperature at the first node; r_{sg} ($0.1\ m^2\ K\ W^{-1}$) is the thermal contact resistance between the skin and the ground surface (Radoń et al., 2014). It was assumed that $T_{g,\ 1}$ is equal to the ground surface temperature (T_g) at the beginning of animal lying down. The net heat flux into interior control volume ($q''_{cond,\ 1}$, $W\ m^{-2}$) of node 1 was calculated as the conduction from the bottom skin minus the conduction to node 2:

$$q''_{cond,\ 1} = q''_{cond,\ s2-g} - (T_{g,\ 1} - T_{g,\ 2}) \Big/ (d_i/2) \quad (29)$$

where $T_{g,\ 2}$ (K) is the underground temperature at node 2. Node spacing was set to be $d_i/2$ for the first and last nodes, and to be d_i for all the other nodes (Bastian et al., 2003). The net heat flux into each interior control volume ($q''_{cond,\ i}$, $W\ m^{-2}$) from nodes i = 2 to 49 was calculated as the conduction input from node i − 1 minus the conduction output to node i + 1:

$$q''_{cond,\ i} = k_{soil}[(T_{g,\ i-1} - T_{g,\ i}) - (T_{g,\ i} - T_{g,\ i+1})] / d_i \quad (30)$$

where k_{soil} ($W\ m^{-1}\ K^{-1}$) is the thermal conductivity of soil; $T_{g,\ i-1}$, $T_{g,\ i}$ and $T_{g,\ i+1}$ (K) are the underground temperature at node i − 1, i and i + 1, respectively. The heat flux at the last node (0.5 m deep underground, $q''_{cond,\ 50}$, $W\ m^{-2}$) was calculated as the conduction input from node 49 minus the conduction output to the adiabatic layer:

$$q''_{cond,\ 50} = k_{soil}[(T_{g,\ 49} - T_{g,\ 50}) - (T_{g,\ 50} - T_{adl})] / (d_i/2) \quad (31)$$

where $T_{g,\ 49}$ (K) the temperature at node 49; $T_{g,\ 50}$ (K) is the temperature at node 50; T_{adl} (K) is the temperature at the adiabatic layer, which was assumed to be a constant equal to the annual average air temperature of the location (Zarrella & De Carli, 2013). It was assumed that heat conduction among the nodes is one-dimensional and shares the same contact area as that between the animal and the ground surface. The net heat flux into each control volume in the soil is equal to the thermal storage in that control volume with time:

$$d(M_{soil}c_{psoil}T_{g,\ i}) / dt = p_c A q''_{cond,\ i} \quad (32)$$

where M_{soil} (kg) is the soil mass for each node; c_{psoil} ($J\ kg^{-1}\ K^{-1}$) is the specific heat capacity of soil. Soil mass can be written as the product of volume and density ($M_{soil} = p_c\ A\ d_i\ \rho_{soil}$), which converts the above equation to:

$$d(\rho_{soil}c_{psoil}T_{g,\ i}d_i) / dt = q''_{cond,\ i} \quad (33)$$

where ρ_{soil} ($kg\ m^{-3}$) is the soil density. Different soil has different thermal properties; here a heavy clay soil with c_{psoil} = 1784 $J\ kg^{-1}\ K^{-1}$, ρ_{soil} = 1784 $kg\ m^{-3}$ and k_{soil} = 1.64 $W\ m^{-1}\ K^{-1}$ was assumed, which is typical in the Central Valley, California, USA (Najib et al., 2020).

3. Model evaluation

Two datasets (Chen et al., 2015; Dikmen & Hansen, 2009) were used to evaluate the predictability of the model for body temperature. Both datasets were collected in the afternoon based on the experimental design. Body temperature data from Dikmen & Hansen (2009) were collected indoor in the afternoon from June to September 2007 in Florida, USA, thus solar radiation was considered to be 0. Measurements were taken over 2 h when the animals were standing up. After removing the data collected from animals exposed to sprinklers, 347 observations from 304 animals were used for evaluation. The dataset from (Chen et al., 2015) is publicly available on the Dryad Digital Repository (Tucker et al., 2020). They collected body temperature data over 1 h when the cows were standing up under the sun in the afternoon from June to August 2011 in California, USA. Only the data collected from animals without any cooling treatment were used (486 observations from 18 animals). Climate data near the animal including air temperature, relative humidity, wind speed and

black globe temperature were recorded when the rectal temperature was measured every 1–3 min for 2 h in the dataset of Dikmen & Hansen (2009) and every 5–10 min for 1 h in the dataset of Chen et al. (2015). The weather data were assumed to change linearly between each time point. The heat production was estimated based on the herd average body weight and milk production. The dataset of Chen et al. (2015) also contained *RR* measurements for all the 486 observations, which were used to compare two *RR* estimation equations (Thompson et al., 2011; Atkins et al., 2018). Both are linear equations regressed on T_b: $RR = 37T_b - 1385$ (Thompson et al., 2011) and $RR = 19.8T_b - 707$ (Atkins et al., 2018), where T_b is in °C and *RR* is in breath min^{-1}.

Correlation between observations and predictions (r^2), root mean squared error of prediction (*RMSEP*) and concordance correlation coefficient (CCC; Lawrence & Lin, 1989) were used to evaluate the accuracy and precision of the model on body temperature and respiration rate estimation.

4. Simulation example

A simulation example was conducted based on a Holstein dairy cow weighing 600 kg, with 176 MJ of metabolisable energy intake per day, producing 25 kg of milk (3.2% of milk protein, 3.5% of milk fat and 4.85% of lactose) per day and having no body weight change. The heat production rate was estimated to be 1240 W based on NRC (2001). Milk production was set to be low because the simulation was conducted under an outdoor environment in hot summer when the animal was likely under heat stress. Three days of simulation were run based on the weather condition in Davis, CA, USA from July 26 to 28, 2019. Hourly air temperature, relative humidity and wind speed were obtained from Weather Underground (Weather Underground, 2019). Weather data were interpolated linearly to provide information of inputs varying on a per second basis (Fig. 2), with the average air temperature, relative humidity and wind speed being 25.8 °C (min = 13.3 °C, max = 37.7 °C), 51.0% (min = 16.0%, max = 95%) and 2.0 m/s (min = 0.67 m s^{-1}, max = 3.8 m s^{-1}), respectively. Annual average temperature in Davis (16.2 °C) was obtained from U.S. Climate Data (U. S. Climate Data, 2021). The timing of animal lying down and standing up is also required to quantify the conduction between animal and ground. In the simulation, we assumed that the animal did not lie down when the ground surface temperature was higher than the lower skin temperature. The proportion of lying down during other time was set based on Drwencke et al. (2020), resulting 7.5 h of lying down per day (details in Supplementary file 2).

5. Sensitivity analysis

Sensitivity measures how influential a parameter is on the model output. A local and a global sensitivity analyses were conducted to estimate the sensitivities of the model parameters. The local sensitivity analysis evaluates the effect of each parameter at a steady state, while the global sensitivity analysis evaluates them dynamically.

5.1. Local sensitivity analysis

In the local sensitivity analysis, 50 model parameters (detailed information in Supplementary file 3), three of which were climate variables (air temperature, relative humidity and wind speed), were analysed. The climate variables were set to nominal values, with air temperature being 34 °C, relative humidity being 18% and wind speed being 2.8 m s^{-1}, which mimicked a typical summer afternoon in Davis, CA, USA. The model was run with the baseline values of all the parameters (p_i, i = 1, …, 50) until the outcome T_b reached a steady state (the outcome does not change more than 0.01% within 1 h). Then the model was rerun twice for each parameter after changing the baseline value by ± 3% (Thompson et al., 2014b) and fixing all the others. The sensitivity S_i (–) for parameter i was calculated as:

$$S_i = \left(\Delta T_{bi} / \Delta T_{pi}\right)\left(\overline{p_i} \Big/ \overline{T_b}\right) \quad (34)$$

where ΔT_{bi} is the change of T_b caused by the change of parameter i (Δp_i), and $\overline{T_b}$ is the outcome of T_b under the baseline value of parameter $\overline{p_i}$. In order to investigate the difference of sensitivity between cows standing up and lying down, two local sensitivity analyses were conducted using the same procedures as described above, except that the animal was assumed to stand up in one analysis while to lie down in the other.

5.2. Global sensitivity analysis

Global sensitivity analysis measured the sensitivity of each parameter throughout a 24 h period based on the method described by Saltelli et al. (2008) and Thompson et al. (2014b). The three climate parameters changed across time and could not be included in the global sensitivity analysis, thus only the rest 47 parameters were included. A parameter matrix X (x_{ij}, $i = 1, \ldots, 10{,}000$ and $j = 1, \ldots, 47$) was constructed with each column representing a parameter and each row representing a simulation. The values for each parameter were drawn from a uniform distribution, with upper and lower bounds given as ± 3% of the baseline value. In total, 10,000 simulations were performed, with the parameter inputs for each simulation given by a row from the parameter matrix. The T_b outputs were saved from each run every 15 min throughout 24 h (96 outcomes in total) and stored in a model output matrix Y (y_{ik}, $i = 1, \ldots, 10{,}000$ and $k = 1, \ldots, 96$).

All columns of the parameter matrix and the output matrix were standardised to X′ and Y′ as:

$$x'_{ij} = \left(x_{ij} - \overline{x_j}\right) / s_{xj} \text{ and } y'_{ik} = \left(y_{ik} - \overline{y}_k\right) \Big/ s_{yk} \quad (35)$$

where $\overline{x}_j$ and s_{xj} are the mean and standard deviation of column j in the parameter matrix X, $\overline{y}_k$ and s_{yk} are the mean standard deviation of column k in the output matrix Y. Then

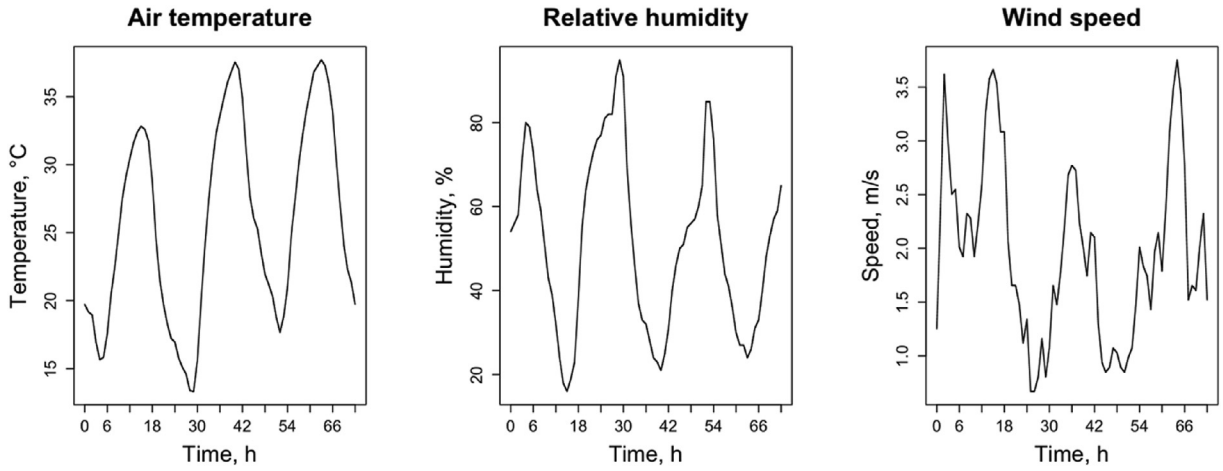

Fig. 2 – Air temperature, relative humidity and wind speed in Davis, CA, USA from July 26 to 28, 2019.

each column of the standardized output matrix was regressed on the standardised parameter matrix as:

$$Y'_k = X'\beta_k + e_k \quad (36)$$

where Y'_k is a vector (10,000 × 1) of column k in the standardized output matrix, X' (10,000 × 47) is the standardised parameter matrix, β_k is a regression coefficient vector (47 × 1), and e_k (10,000 × 1) is a residual vector.

In a standardised regression setting, the total variation of the output equals one and the sensitivity of a parameter can be represented by its regression coefficient squared, which describes the fraction of the model variance that is accounted for by variation of the parameter. As a result, each parameter had 96 sensitivities corresponding to each time point. The R^2, the coefficient of determination, from the standardised regression will be close to 1 if the model is linear in its parameters. The global sensitivity analysis was conducted using the same lying time as that in the simulation, and climate condition in Davis, CA, USA on July 26, 2019.

6. Results and discussion

6.1. Model evaluation

The *RMSEP* of the thermal balance model prediction of body temperature on the data from Dikmen & Hansen (2009) was 1.16 °C (2.9% of the observation mean), while the data from Chen et al. (2015) was 0.40 °C (1.0% of the observation mean). The prediction on the data from Dikmen & Hansen (2009) had lower r^2 (0.43 vs 0.91, respectively) and *CCC* (0.36 vs 0.79, respectively) than the data from Chen et al. (2015). Figure 3 suggests that the model was likely to overestimate the body temperature for both datasets, given many predictions were higher than the observations. Cows stood indoor for 2 h in Dikmen & Hansen (2009) while cows were forced to stand under the sun for 1 h in Chen et al. (2015) when sampling, which resulted in a higher average body temperature from Chen et al. (2015) than that from Dikmen & Hansen (2009). The variance of the body temperature in the dataset of Dikmen & Hansen (2009) was 0.62, while that in the dataset of Chen et al. (2015) was 0.39. The thermal balance model fitted the dataset from Chen et al. (2015) better, probably because Dikmen & Hansen (2009) collected 347 observations from 304 animals, which resulted in a larger animal variation. In contrast, Chen et al. (2015) collected 486 observations of body temperature from 18 animals consecutively, which can be better described by our model. However, data from cows lying down was not available, so the evaluation of the conduction between the animal and ground requires appropriate measurements to be made in the future.

For respiration rate prediction (Fig. 4), the equation from Thompson et al. (2011) had a similar *RMSEP* (25.0 vs 23.5 breath s^{-1}, respectively; 26.4% vs 24.8% of the observation mean, respectively) as the one from Atkins et al. (2018), but a greater *CCC* value (0.45 vs 0.33, respectively). Both equations predict respiration rate by a linear regression on body temperature, thus had the same r^2 of 0.66. Thompson's equation had a slightly larger *RMSEP* but a better *CCC* value, thus was used in our model. Thompson's equation was derived through a meta-analysis using data from *Bos taurus* cattle, which included animals other than dairy cows (Thompson et al., 2011), while Atkins's equation was developed based on an animal trial using only 8 cows (Atkins et al., 2018). Both equations may not be accurate enough, therefore a meta-analysis on dairy cattle respiration rate should be conducted in the future to refine the respiration rate equation.

6.2. Simulation example

The simulated temperature of body core, skin and coat is shown in Fig. 5. The average temperatures of body, top and bottom skin, and top and bottom coat were 40.9 °C (min = 39.0 °C, max = 42.1 °C), 35.6 °C (min = 32.5 °C, max = 38.6 °C), 35.9 °C (min = 32.5 °C, max = 40.8 °C), 34.1 °C (min = 21.6 °C, max = 48.1 °C) and 33.7 °C (min = 21.7 °C, max = 40.8 °C), respectively. The body temperature was higher than normal (38.5 °C), probably due to the assumption that the animal was unshaded and had no access to any cooling

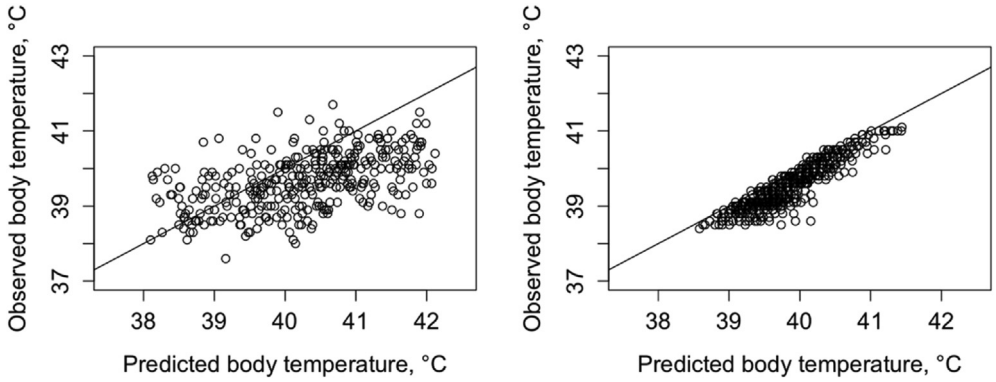

Fig. 3 – Observed body temperatures from Dikmen & Hansen (2009; left) and Chen et al. (2015; right) against predicted body temperatures based on the thermal balance model. The solid line represents a perfect prediction.

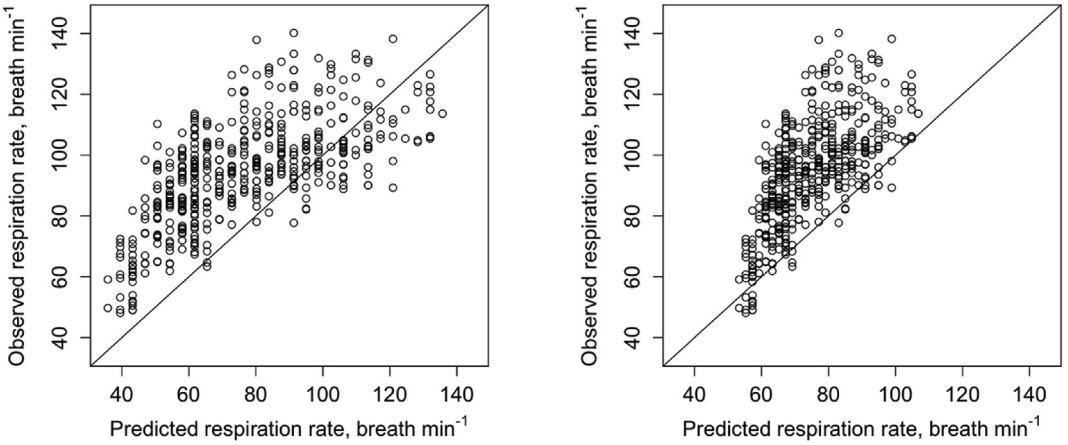

Fig. 4 – Observed respiration rate from Chen et al. (2015) against predicted respiration rate based on $y = 37x - 1385$ (Thompson et al., 2011; left) and $y = 19.8x - 707$ (Atkins et al., 2018; right), where x is body temperature (°C) and y is respiration rate (breath min^{-1}). The solid line represents a perfect prediction.

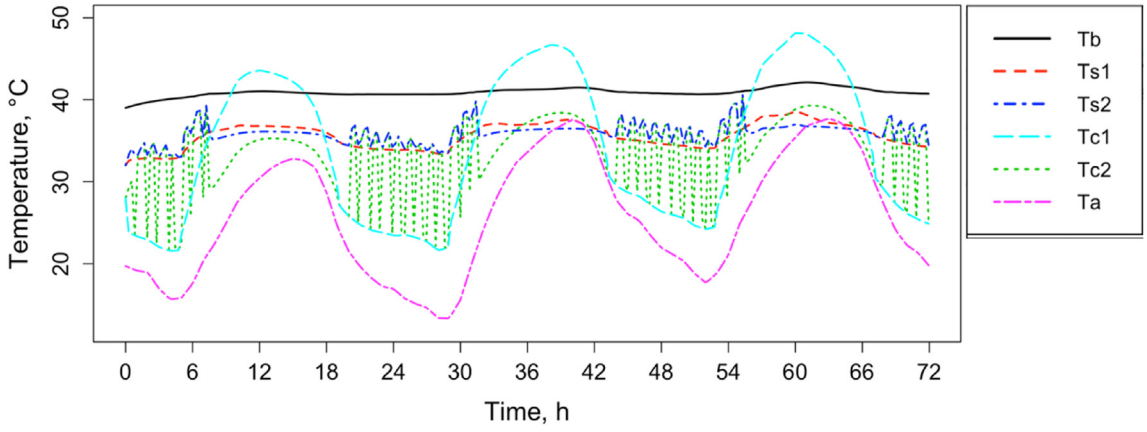

Fig. 5 – Simulation of body temperature (T_b), top (T_{s1}) and bottom (T_{s2}) skin temperature, and top (T_{c1}) and bottom (T_{c2}) coat temperature based on the air temperature (T_a), relative humidity and wind speed in Davis, CA, USA from July 26 to 28, 2019.

equipment (roofs, fans or sprinklers). The variation of body core temperature is the smallest, followed by skin temperature, and coat temperature. The body temperature oscillated every 24 h, with the peak occurring around 16:00 to 17:00 h and the minimum occurring around 04:00 to 05:00 h. The top skin and coat temperatures followed the same pattern, with the peak occurring around 3 h earlier and the minimum occurring 1 h earlier than the body temperature. Environmentally, the peak temperature of top coat and skin temperatures occurred around 1 h after the solar radiation peak, while body

temperature reached a peak around 1 h after peak air temperature. A similar pattern was also reported by Scott et al. (1983), indicating the process of heat accumulation. The bottom skin and coat temperature changed periodically because of lying down and standing up. When the animal lay down, the bottom skin temperature was higher than the top skin temperature due to lack of evaporation. After the animal stood up, the bottom skin and coat temperature gradually changed to become the same as the top skin and coat temperature due to the same heat transfer mechanism occurring to both top and bottom parts. However, when the ground surface temperature was higher than the bottom skin temperature, the animal remained standing and the bottom skin and coat temperatures were lower than the top ones because of the stronger solar radiation received by the top coat.

The relevant proportions of five mechanisms of heat dissipation are shown in Table 1. Evaporation accounted for 48.0% of the total amount of dissipated heat on average throughout the simulation, followed by long wave radiation (18.2%), respiration (16.2%), convection (14.9%), and conduction (2.7%). Figure 6 shows the heat flux over the three days. Evaporation, convection, solar radiation and long wave radiation are shown as the weighted average heat flux at the top and bottom nodes (e.g., evaporation = 0.8 evaporation at the top skin + 0.2 evaporation at the bottom skin). Solar radiation was an important heat source, thus shading is essential in summer to prevent heat stress. Evaporation was the major way to dissipate heat in the afternoon when the air temperature was high and relative humidity was low, which is also suggested by previous studies (McGovern & Bruce, 2000; Thompson et al., 2014a). Heat dissipation through respiration followed a similar pattern as air temperature while long wave radiation showed an opposite pattern to air temperature, because respiration is mainly dependent on the air temperature and body temperature whilst long wave radiation depends on the difference between coat temperature and surrounding radiant temperature, which was smaller at noon and larger at midnight. Heat convection increased when solar radiation increased, because coat temperature increased due to solar radiation and caused a larger driving temperature difference for convection from the coat surface. Heat conduction between the animal and ground surface accounted for a very low percentage of the total heat dissipation, because only 20% of the animal surface is in contact with the ground when lying down (Ortiz et al., 2015). Based on our assumptions, the animal did not lie down during most of the daytime when the temperature of ground surface was higher than skin temperature. Although the total heat dissipation through conduction was small, the heat flux element showed a peak each time when the animal lay down between midnight and sunrise. This agrees with Bastian et al. (2003) who reported significant heat dissipation through conduction when the ground temperature is low.

6.3. *Sensitivity analysis*

Local sensitivities of the top 10 parameters are shown in Fig. 7. Two analyses shared the same top 10 parameters with small differences in the rank. Air temperature was the most

Table 1 – – The average percentage (%) of heat dissipation (J) through convection, evaporation, long wave radiation, respiration and conduction between animal and ground surface to the sum of them during different time periods for the simulation based on the weather condition in Davis, CA, USA from July 26 to 28, 2019.

	00:00 to 06:00 h	06:00 to 12:00 h	12:00 to 18:00 h	18:00 to 24:00 h	Entire day
Convection	14.1	19.8	14.9	8.0	14.9
Evaporation	32.6	49.3	57.0	45.7	48.0
Long wave radiation	28.7	16.6	11.5	21.8	18.2
Respiration	15.9	13.8	16.6	19.7	16.2
Conduction	8.7	0.5	–	4.8	2.7

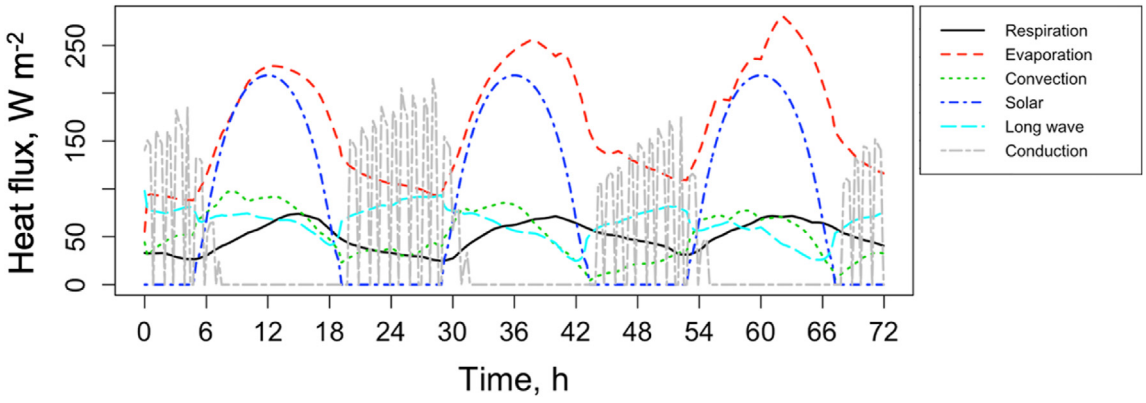

Fig. 6 – Simulated heat flux of respiration, evaporation, convection, solar radiation, long wave radiation and conduction between animal and ground based on the weather condition in Davis, CA, USA from July 26 to 28, 2019. Evaporation, convection, solar radiation, and long wave radiation are shown as the weighted average heat flux (e.g., evaporation = 0.8 evaporation at the top skin +0.2 evaporation at the bottom skin) at the bottom and top nodes.

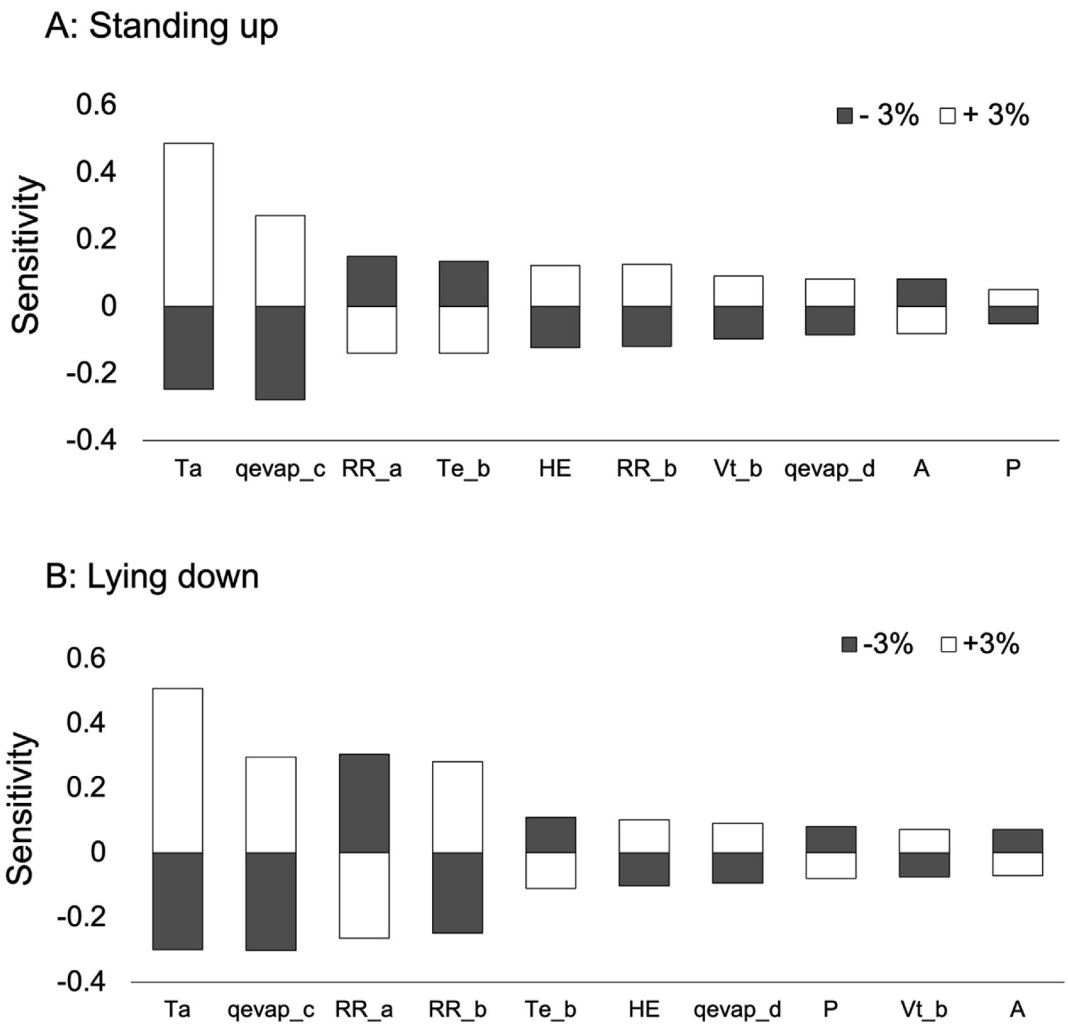

Fig. 7 – Top 10 sensitive parameters in the local sensitivity analyses for a dairy cow standing up (A) and lying down (B) when changing the parameters ± 3%. *Ta* = Air temperature (K), *qevap_c* = Parameter *c* for evaporation rate (–), *RR_a* = Parameter a for respiration rate (–), *Te_b* = Parameter b for exhaled air temperature, *HE* = Heat production (W), *RR_b* = Parameter b for respiration rate (–), *Vt_b* = Parameter b for tidal volume (–), *qevap_d* = Parameter *d* for evaporation rate (–), *A* = Animal surface area (m^2), *P* = Air pressure (Pa).

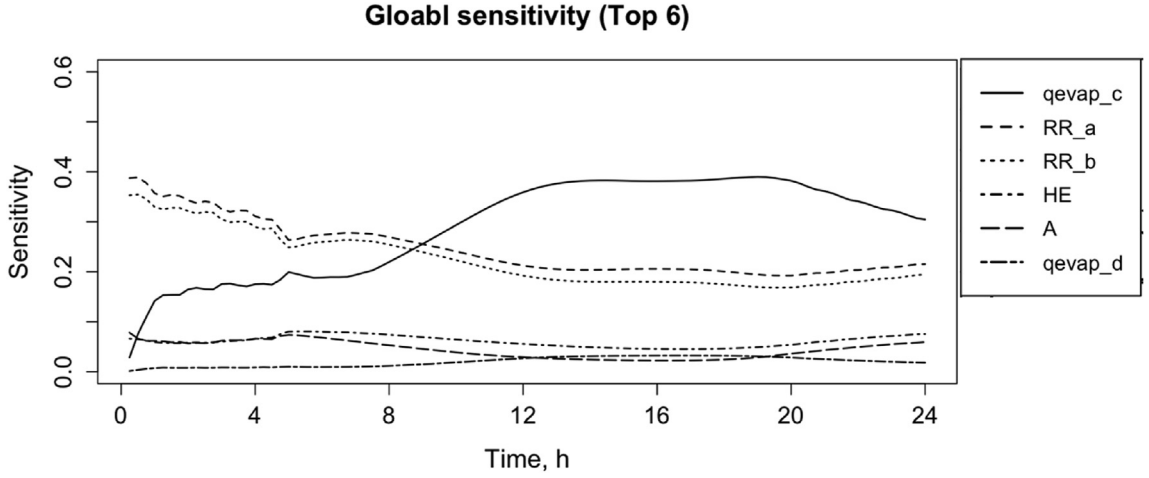

Fig. 8 – Global sensitivity (Top 6) of the parameters throughout 24 h *qevap_c* = Parameter *c* for evaporation rate (–), *RR_a* = Parameter *a* for respiration rate (–), *RR_b* = Parameter *b* for respiration rate (–), *HE* = Heat production (W), *A* = Animal surface area (m^2), *qevap_d* = Parameter *d* for evaporation rate (–).

sensitive amongst the 10 parameters for both animal standing up and lying down. Also, two parameters related to heat evaporation (*qevap_c* and *qevap_d*) and four parameters related to respiration (*RR_a, RR_b, Vt_b* and *Te_b*) were also sensitive for both situations when animals were standing up and lying down. The other three top 10 sensitive parameters were heat production, surface area and air pressure, probably because heat production and surface area were in the differential equations and directly determine the gain and loss of heat, and air pressure was used to calculate multiple heat transfer mechanisms, including conduction, evaporation and respiration. The average R^2 of the regressions in the global sensitivity analysis was 0.96, indicating that the heat balance model was linear in the parameters and regression was a valid technique to investigate the global sensitivities. Six parameters with minimum global sensitivity greater than 0.05 are shown in Fig. 8. Two respiration parameters were the most sensitive before around 08:00 h, while the evaporation rate parameter became the most sensitive afterwards. All the six parameters were also within the top 10 local sensitivities.

The sensitivity analysis suggested that the parameters related to respiration and heat evaporation through sweating were well quantified since small changes in those parameters can change the outcome considerably. Most of these parameters were derived from either old or small datasets, thus re-evaluation of them with a large and recent dataset may improve the model accuracy and resolve the model overestimation. Heat production is assumed to be constant in our model, which does not account for the heat increment effect of feeding (Sprinkle et al., 2000). In addition, heat stress induces behavioural and metabolic changes in cattle including reduced dry matter intake, selective consumption and reduced heat production (Fox & Tylutki, 1998), while the estimation of heat production in our model is based on a non-stressed condition. Since heat production is also a sensitive parameter, the bias of the overall heat production estimation may impact the model outcome. Also, the long-term effect of heat stress and resulting physiological changes were not considered in our model, and if incorporated, may change the sensitivity values.

7. Conclusions

A dynamic model describing the thermal balance of Holstein dairy cattle was developed in this study. Heat production by the animal, heat conduction among the body core, skin and coat, and heat flows between the animal and the environment, including conduction, convection, evaporation and radiation were considered. Based on experimental results from two datasets, the model overestimates body temperature. This may be resolved by re-evaluating several sensitive parameters including respiration and evaporation coefficients using more recent data. Thus, despite some limitations, the thermal balance model can provide a guideline on the thermal condition of the animal under hot climate and a mechanistic modelling framework for future studies.

Our future work will focus on evaluating and guiding the use of cooling strategies based on the thermal balance model.

Declaration of competing interest

The authors declare that they have no known competing financial interests or personal relationships that could have appeared to influence the work reported in this paper.

Acknowledgements

This research was supported in part by the W. K. Kellogg Endowment and USDA National Institute of Food and Agriculture (Washington, DC) Multistate Research Project NC-2040. We gratefully acknowledge the infrastructure support of the Department of Animal Science, College of Agricultural and Environmental Sciences, and the California Agricultural Experiment Station of the University of California, Davis, CA, USA. We are grateful to Drs. Peter J. Hansen (University of Florida, FL, USA), Jennifer Van Os (University of Wisconsin, Madison, WI, USA), and Cassandra B. Tucker (University of California, Davis, CA, USA) for generously sharing their experimental data.

Appendix A. Supplementary data

Supplementary data related to this article can be found at https://doi.org/10.1016/j.biosystemseng.2021.06.009.

REFERENCES

Araki, C. T., Nakamura, R. M., Kam, L. W. G., & Clarke, N. (1984). Effect of lactation on diurnal temperature patterns of dairy cattle in hot environments. *Journal of Dairy Science, 67*(8), 1752–1760. https://doi.org/10.3168/jds.S0022-0302(84)81501-5

Atkins, I. K., Cook, N. B., Mondaca, M. R., & Choi, C. Y. (2018). Continuous respiration rate measurement of heat–stressed dairy cows and relation to environment, body temperature, and lying time. *Transactions of the ASAE, 61*(5), 1475–1485. https://doi.org/10.13031/trans.12451

Baker, C. C., Coppock, C. E., Lanham, J. K., Nave, D. H., Labore, J. M., Brasington, C. F., & Stermer, R. A. (1988). Chilled drinking water effects on lactating Holstein cows in summer. *Journal of Dairy Science, 71*(10), 2699–2708. https://doi.org/10.3168/jds.S0022-0302(88)79863-X

Bastian, K. R., Gebremedhin, K. G., & Scott, N. R. (2003). A finite difference model to determine conduction heat loss to a water-filled mattress for dairy cows. *Transactions of the ASAE, 46*(3), 773–780. https://doi.org/10.13031/2013.13592

Bergman, T. L., Incropera, F. P., Lavine, A. S., & Dewitt, D. P. (2011). *Introduction to heat transfer*. John Wiley & Sons (Chapter 5).

Berman, A. (2006). Extending the potential of evaporative cooling for heat–stress relief. *Journal of Dairy Science, 89*(10), 3817–3825. https://doi.org/10.3168/jds.S0022-0302(06)72423-7

Bertipaglia, E. C. A., Silva, R. G., & Maia, A. S. C. (2005). Fertility and hair coat characteristics of Holstein cows in a tropical environment. *Animal Reproduction, 2*(3), 187–194.

Bewley, J. M., Grott, M. W., Einstein, M. E., & Schutz, M. M. (2008). Impact of intake water temperatures on reticular temperatures of lactating dairy cows. *Journal of Dairy Science, 91*(10), 3880–3887. https://doi.org/10.3168/jds.2008-1159

Chen, J. M., Schütz, K. E., & Tucker, C. B. (2015). Cooling cows efficiently with sprinklers: Physiological responses to water spray. *Journal of Dairy Science, 98*(10), 6925–6938. https://doi.org/10.3168/jds.2015-9434

Chen, J. M., Schütz, K. E., & Tucker, C. B. (2016). Cooling cows efficiently with water spray: Behavioral, physiological, and production responses to sprinklers at the feed bunk. *Journal of Dairy Science, 99*(6), 4607–4618. https://doi.org/10.3168/jds.2015-10714

Cook, N. B., Mentink, R. L., Bennett, T. B., & Burgi, K. (2007). The effect of heat stress and lameness on time budgets of lactating dairy cows. *Journal of Dairy Science, 90*(4), 1674–1682. https://doi.org/10.3168/jds.2006-634

Das, R., Sailo, L., Verma, N., Bharti, P., & Saikia, J. (2016). Impact of heat stress on health and performance of dairy animals: A review. *Veterinary World, 9*(3), 260. https://doi.org/10.14202/vetworld.2016.260-268

da Silva, R. G., LaScala, N., Lima Filho, A., & Catharin, M. (2002). Respiratory heat loss in the sheep: A comprehensive model. *Journal of Biometeorology, 46*(3), 136–140. https://doi.org/10.1007/s00484-002-0128-0

Dikmen, S., & Hansen, P. J. (2009). Is the temperature-humidity index the best indicator of heat stress in lactating dairy cows in a subtropical environment? *Journal of Dairy Science, 92*(1), 109–116. https://doi.org/10.3168/jds.2008-1370

Drwencke, A. M., Tresoldi, G., Stevens, M. M., Narayanan, V., Carrazco, A. V., Mitloehner, F. M., Pistochini, T. E., & Tucker, C. B. (2020). Innovative cooling strategies: Dairy cow responses and water and energy use. *Journal of Dairy Science, 103*(6), 5440–5454. https://doi.org/10.3168/jds.2019-17351

Fox, D. G., & Tylutki, T. P. (1998). Accounting for the effects of environment on the nutrient requirements of dairy cattle. *Journal of Dairy Science, 81*(11), 3085–3095. https://doi.org/10.3168/jds.S0022-0302(98)75873-4

Gebremedhin, K. G., & Wu, B. (2001). A model of evaporative cooling of wet skin surface and Fur layer. *Journal of Thermal Biology, 26*(6), 537–545. https://doi.org/10.1016/S0306-4565(00)00048-6

Gebremedhin, K. G., Wu, B., & Perano, K. (2016). Modeling conductive cooling for thermally stressed dairy cows. *Journal of Thermal Biology, 56*, 91–99. https://doi.org/10.1016/j.jtherbio.2016.01.004

Hansen, P. J. (2020). Prospects for gene introgression or gene editing as a strategy for reduction of the impact of heat stress on production and reproduction in cattle. *Theriogenology, 154*, 190–202. https://doi.org/10.1016/j.theriogenology.2020.05.010

Hottel, H. C. (1976). A simple model for estimating the transmittance of direct solar radiation through clear atmospheres. *Solar Energy, 18*(2), 129–134. https://doi.org/10.1016/0038-092X(76)90045-1

Igono, M. O., Bjotvedt, G., & Sanford-Crane, H. T. (1992). Environmental profile and critical temperature effects on milk production of Holstein cows in desert climate. *International Journal of Biometeorology, 36*(2), 77–87. https://doi.org/10.1007/BF01208917

Kuehn, L. A., Stubbs, R. A., & Weaver, R. S. (1970). Theory of the globe thermometer. *Journal of Applied Physiology, 29*(5), 750–757. https://doi.org/10.1152/jappl.1970.29.5.750

Lacetera, N., Bernabucci, U., Ronchi, B., & Nardone, A. (1996). Body condition score, metabolic status and milk production of early lactating dairy cows exposed to warm environment. *Rivista di Agricoltura Subtropicale e Tropicale, 90*(1), 43–55.

Lawrence, I., & Lin, K. (1989). A concordance correlation coefficient to evaluate reproducibility. *Biometrics, 45*, 255–268. https://doi.org/10.2307/2532051

Mader, T. L., Davis, M. S., & Brown-Brandl, T. (2006). Environmental factors influencing heat stress in feedlot cattle. *Journal of Animal Science, 84*(3), 712–719. https://doi.org/10.2527/2006.843712x

Maia, A. S. C., DaSilva, R. G., & Loureiro, C. M. B. (2005). Respiratory heat loss of Holstein cows in a tropical environment. *International Journal of Biometeorology, 49*(5), 332–336. https://doi.org/10.1007/s00484-004-0244-0

Maia, A. S. C., & Loureiro, C. B. (2005). Sensible and latent heat loss from the body surface of Holstein cows in a tropical environment. *International Journal of Biometeorology, 50*(1), 17–22. https://doi.org/10.1007/s00484-005-0267-1

McArthur, A. J. (1987). Thermal interaction between animal and microclimate: A comprehensive model. *Journal of Thermal Biology, 126*(2), 203–238. https://doi.org/10.1016/S0022-5193(87)80229-1

McGovern, R. E., & Bruce, J. M. (2000). AP—animal production technology: A model of the thermal balance for cattle in hot conditions. *Journal of Agricultural Engineering Research, 77*(1), 81–92. https://doi.org/10.1006/jaer.2000.0560

Monteith, J., & Unsworth, M. (2013). *Principles of environmental physics: Plants, animals, and the atmosphere*. Oxford, UK: Academic Press.

Nabenishi, H., Ohta, H., Nishimoto, T., Morita, T., Ashizawa, K., & Tsuzuki, Y. (2011). Effect of the temperature-humidity index on body temperature and conception rate of lactating dairy cows in southwestern Japan. *Journal of Reproduction and Development*. https://doi.org/10.1262/jrd.10-135T, 1104050364–1104050364.

Najib, A., Zarrella, A., Narayanan, V., Bourne, R., & Harrington, C. (2020). Techno-economic parametric analysis of large diameter shallow ground heat exchanger in California climates. *Energy and Buildings, 228*, 110444. https://doi.org/10.1016/j.enbuild.2020.110444

Nardone, A., Ronchi, B., Lacetera, N., Ranieri, M. S., & Bernabucci, U. (2010). Effects of climate changes on animal production and sustainability of livestock systems. *Livestock Science, 130*, 57–69. https://doi.org/10.1016/j.livsci.2010.02.011

NRC. (2001). *Nutrient requirements of dairy cattle* (7th ed.). Washington, DC: National Academy Press.

Ortiz, X. A., Smith, J. F., Rojano, F., Choi, C. Y., Bruer, J., Steele, T., Schuring, N., Allen, J., & Collier, R. J. (2015). Evaluation of conductive cooling of lactating dairy cows under controlled environmental conditions. *Journal of Dairy Science, 98*(3), 1759–1771. https://doi.org/10.3168/jds.2014-8583

Purwanto, B. P., Abo, Y., Sakamoto, R., Furumoto, F., & Yamamoto, S. (1990). Diurnal patterns of heat production and heart rate under thermoneutral conditions in Holstein Friesian cows differing in milk production. *The Journal of Agricultural Science, 114*(2), 139–142. https://doi.org/10.1017/S0021859600072117

R Core Team. (2019). *R: A language and environment for statistical computing*. Vienna, Austria: R Foundation for Statistical Computing.

Radoń, J., Bieda, W., Lendelová, J., & Pogran, Š. (2014). Computational model of heat exchange between dairy cow and bedding. *Computers and Electronics in Agriculture, 107*, 29–37. https://doi.org/10.1016/j.compag.2014.06.006

Roenfeldt, S. (1998). You can't afford to ignore heat stress. *Dairy Herd Management, 35*, 6–12.

Roth, Z., Meidan, R., Braw-Tal, R., & Wolfenson, D. (2000). Immediate and delayed effects of heat stress on follicular development and its association with plasma FSH and inhibin concentration in cows. *Journal of Reproduction and Fertility, 120*(1), 83–90. https://doi.org/10.1530/reprod/120.1.83

Saltelli, A., Ratto, M., Andres, T., Campolongo, F., Cariboni, J., Gatelli, D., Saisana, M., & Tarantola, S. (2008). *Global sensitivity analysis: The primer*. West Sussex, England: John Wiley & Sons.

Scott, I. M., Johnson, H. D., & Hahn, G. L. (1983). Effect of programmed diurnal temperature cycles on plasma thyroxine level, body temperature, and feed intake of Holstein dairy cows. *International Journal of Biometeorology, 27*(1), 47–62. https://doi.org/10.1007/BF02186300

Shultz, T. A. (1984). Weather and shade effects on cow corral activities. *Journal of Dairy Science, 67*(4), 868–873. https://doi.org/10.3168/jds.S0022-0302(84)81379-X

Silva, R. G. D., & Maia, A. S. C. (2011). Evaporative cooling and cutaneous surface temperature of Holstein cows in tropical conditions. *Revista Brasileira de Zootecnia, 40*(5), 1143–1147. https://doi.org/10.1590/S1516-35982011000500028

Soetaert, K., & Petzoldt, T. (2010). Inverse modelling, sensitivity and Monte Carlo analysis in R using package FME. *Journal of Statistical Software, 33*(3), 1–28. https://doi.org/10.18637/jss.v033.i03

Sprinkle, J. E., Holloway, J. W., Warrington, B. G., Ellist, W. C., Stuth, J. W., Forbes, T. D. A., & Greene, L. W. (2000). Digesta kinetics, energy intake, grazing behavior, and body temperature of grazing beef cattle differing in adaptation to heat. *Journal of Animal Science, 78*(6), 1608–1624. https://doi.org/10.2527/2000.7861608x

Thompson, V. A., Barioni, L. G., Rumsey, T. R., Fadel, J. G., & Sainz, R. D. (2014a). The development of a dynamic, mechanistic, thermal balance model for Bos indicus and Bos taurus. *The Journal of Agricultural Science, 152*(3), 464. https://doi.org/10.1017/S002185961300049X

Thompson, V. A., Fadel, J. G., & Sainz, R. D. (2011). Meta-analysis to predict sweating and respiration rates for Bos indicus, Bos taurus, and their crossbreds. *Journal of Animal Science, 89*(12), 3973–3982. https://doi.org/10.2527/jas.2011-3913

Thompson, V. A., Sainz, R. D., Strathe, A. B., Rumsey, T. R., & Fadel, J. G. (2014b). The evaluation of a dynamic, mechanistic, thermal balance model for Bos indicus and Bos taurus. *The Journal of Agricultural Science, 152*(3), 483. https://doi.org/10.1017/S0021859613000506

Thorsson, S., Lindberg, F., Eliasson, I., & Holmer, B. (2007). Different methods for estimating the mean radiant temperature in an outdoor urban setting. *International Journal of Climatology: A Journal of the Royal Meteorological Society, 27*(14), 1983–1993. https://doi.org/10.1002/joc.1537

Tucker, C. B., Schütz, K. E., & Jennifer, M. (2020). Data from: Cooling cows efficiently with sprinklers: physiological responses to water spray. *Dryad Digital Repository*. https://doi.org/10.25338/B88P7H

Turnpenny, J. R., McArthur, A. J., Clark, J. A., & Wathes, C. M. (2000a). Thermal balance of livestock: 1. A parsimonious model. *Agricultural and Forest Meteorology, 101*(1), 15–27. https://doi.org/10.1016/S0168-1923(99)00159-8

Turnpenny, J. R., Wathes, C. M., Clark, J. A., & McArthur, A. J. (2000b). Thermal balance of livestock: 2. Applications of a parsimonious model. *Agricultural and Forest Meteorology, 101*(1), 29–52. https://doi.org/10.1016/S0168-1923(99)00157-4

Weather Underground. Davis, CA weather condition. (2019). https://www.wunderground.com/weather/us/ca/davis. (Accessed 29 July 2019).

U. S. Climate Data. Climate Davis – California. (2021). https://www.usclimatedata.com/climate/davis/california/united-states/usca0284. (Accessed 3 April 2021).

West, J. W. (2003). Effects of heat-stress on production in dairy cattle. *Journal of Dairy Science, 86*(6), 2131–2144. https://doi.org/10.3168/jds.S0022-0302(03)73803-X

Yamamoto, S., Young, B. A., Purwanto, B. P., Nakamasu, F., & Matsumoto, T. (1994). Effect of solar radiation on the heat load of dairy heifers. *Australian Journal of Agricultural Research, 45*(8), 1741–1749. https://doi.org/10.1071/AR9941741

Zarrella, A., & De Carli, M. (2013). Heat transfer analysis of short helical borehole heat exchangers. *Applied Energy, 102*, 1477–1491. https://doi.org/10.1016/j.apenergy.2012.09.012

Zimbelman, R. B., Rhoads, R. P., Rhoads, M. L., Duff, G. C., Baumgard, L. H., & Collier, R. J. (2009). A re-evaluation of the impact of temperature humidity index (THI) and black globe humidity index (BGHI) on milk production in high producing dairy cows. *Proceedings of the 24th Southwest Nutrition and Management conference*, 158–169.